Dynamic Stability and Levation Control in Maglev Systems

P. Sayegh,* H. Déo,† and Y. Abou Rabii‡
École Polytechnique, Route de Saclay, 91120 Palaiseau, France

A. Couairon§
Centre de Physique Theorique (CPhT), CNRS, Ecole Polytechnique, F-91128 Palaiseau, France

All authors contributed equally to this work.

This work provides tools for optimizing the stability and levitation of Maglev trains. To optimize passenger capacity, we derive an expression for levitation height as a function of additional weight, refining this model by fitting free parameters to a scaled-down experimental Electromagnetic Suspension (EMS) train. We construct a mathematical model for an Electrodynamic Suspension (EDS) Maglev system, and develop the analytical expressions that describe the system's behavior, ultimately simulating them under standard and extreme conditions. This approach accurately predicts levitation dynamics, with applications toward safer and more efficient Maglev systems and offers groundwork for further stability and load capacity improvements.

1. INTRODUCTION

Magnetic Levitation (Maglev) technology enables contactless suspension and propulsion, offering significant potential to revolutionize transportation by reducing friction and enhancing speed and stability. However, a major challenge lies in optimizing stability and levitation to improve safety and efficiency under diverse conditions. Maglev systems are broadly classified into Electromagnetic Suspension (EMS), which relies on attractive magnetic forces for levitation, and Electrodynamic Suspension (EDS), which uses repulsive forces induced by currents in conductive guideways.

In this paper, we investigate a simplified EMS system through experimentation and theoretical modeling. By fitting experimental data, we derive an expression for levitation height as a function of mass to optimize the train's capacity. Additionally, we develop a theoretical model of the EDS system to analyze levitation dynamics, including equilibrium height under various conditions. The results demonstrate that the model effectively simulates the system and maintains levitation under extreme scenarios. Together, these contributions advance the understanding of Maglev systems, paving the way for safer and more efficient designs.

2. PRINCIPLES OF MAGNETIC LEVITATION

Magnetic levitation (Maglev) systems leverage electromagnetic forces to achieve contactless suspension and propulsion. These forces enable frictionless motion, allowing Maglev systems to operate with minimal mechanical wear and reduced energy losses. The fundamental principles governing Maglev systems are rooted in electromagnetic interactions, including force generation, stability, and levitation dynamics.

2.1. General Theory

Maglev systems rely on electromagnetic forces to counteract gravitational forces and achieve stable suspension. The net force on the levitating body can be described as:

$$F_{\text{net}} = F_{\text{mag}} - F_{\text{grav}}, \tag{1}$$

where F_{mag} is the upward magnetic force, and $F_{\text{grav}} = mg$ is the downward gravitational force, with m as the mass of the levitating object and g as the acceleration due to gravity.

For stable levitation, the system must satisfy:

$$F_{\text{mag}} = F_{\text{grav}}, \tag{2}$$

ensuring equilibrium at a specific levitation height. However, Earnshaw's Theorem states that it is impossible for a static arrangement of charges or magnets to achieve stable equilibrium through purely electrostatic or magnetostatic forces. This implies that additional mechanisms—such as dynamic stabilization or the use of diamagnetic or induced currents—are required to achieve levitation.

Stability depends on the system's ability to restore equilibrium when perturbed. This requires a dynamic variation in the magnetic force, typically achieved through active control (in EMS systems) or passive stabilization (in EDS systems). The condition for stability is quantified by analyzing the vertical force gradient:

$$\frac{\partial F_{\text{mag}}}{\partial z} > 0, \tag{3}$$

where z is the vertical displacement. A positive gradient ensures that an upward displacement reduces the net force, pulling the body back toward equilibrium.

* peter.sayegh@polytechnique.edu
† hadrien.deo@polytechnique.edu
‡ yazan.abou-rabii@polytechnique.edu
§ arnaud.couairon@polytechnique.edu

2.2. Differences Between EMS and EDS

Electromagnetic Suspension (EMS) systems achieve levitation through attractive forces between electromagnets on the vehicle and ferromagnetic materials on the guideway. The electromagnets are actively controlled to maintain stability, as the inherently unstable nature of attractive forces—dictated by Earnshaw's Theorem—requires constant feedback adjustments. EMS systems typically operate with a small levitation gap, on the order of millimeters.

In contrast, Electrodynamic Suspension (EDS) systems rely on repulsive forces generated by induced currents in conductive guideways. The magnetic fields from the train's magnets induce eddy currents in the guideway, creating a repulsive force. This approach circumvents Earnshaw's Theorem by utilizing dynamic magnetic fields and induced currents. EDS systems are passively stable for vertical displacements, as the restoring forces increase with distance. This allows for a larger levitation gap, typically in the range of several centimeters.

While EMS systems require precise active control to counteract instabilities, EDS systems exhibit inherent stability but depend on the vehicle's speed to generate sufficient levitation forces. These differences influence their respective applications and design trade-offs, but both systems share common principles of electromagnetic force generation and stability dynamics.

3. EXPERIMENTAL SETUP

3.1. The Scaled-Down Maglev Train Experiment

A scaled-down Maglev train model was constructed to investigate how the levitation height of the train changes with added mass. The train's base was a wooden block with dimensions of 12 cm (length), 5 cm (width), and 2 cm (height), fitted with Neodymium magnets on its underside. These magnets interacted with magnetic tape laid on the track to achieve levitation. The total mass of the train, including the magnets and wooden block, was $m_0 = 62 \pm 1$ g. The uncertainty in mass measurements is attributed to the precision of the weighing scale used.

The track consisted of a 50 cm strip of magnetic tape attached to a cardboard base, with a width of 8 cm. To maintain lateral stability, 90-degree angle pieces were affixed to the edges of the track, preventing the train from sliding during experimentation. A key component of the setup was the use of monopolar magnetic tape. Since only bipolar tape is commercially available, we repolarized the tape by rubbing it with Neodymium magnets to align its magnetic domains, effectively creating a monopolar effect.

The experimental procedure involved gluing two strips of repolarized magnetic tape onto the underside of the train to form the levitating mechanism. Similarly, two long strips of magnetic tape were affixed to the track to act as rails, with the same monopolar alignment. This configuration ensured stable levitation for the experiment.

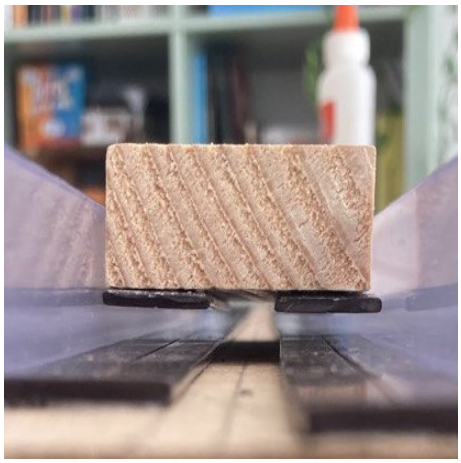

Figure 1. Experimental Maglev Train

3.2. Measurement of Levitation Height

To study the effect of mass on levitation height, a lightweight cardboard cup was placed on top of the train to hold additional weights. Rice was used as an adjustable weight source, allowing precise increments of mass to be added. The mass of the system was measured using a weighing scale with a precision of 1 g, leading to a measurement uncertainty of $u(m) = \pm 1$ g. Levitation height was measured using a ruler with a resolution of 1 mm, and the corresponding uncertainty was taken as $u(h) = \pm 0.5$ mm, accounting for observer error.

The experimental data for levitation height (h) and mass (m) are summarized in Table 1 (Appendix A). These measurements formed the basis for further theoretical modeling and analysis.

3.3. Force Derivation and Theoretical Fitting

The relationship between the levitation height (h) and added mass (m) was derived by modeling the forces acting on the train. To simplify calculations, we assumed the lower and upper magnets were perfectly aligned, neglecting diagonal forces, and treated the thickness of the magnets as negligible compared to the train's height. The geometry used in this derivation is shown in Fig. 8.

The magnetic force exerted by the guideway on the train in the vertical direction (z) was computed by considering the magnetic dipole interaction. The magnets were modeled as infinitesimal layers of dipoles with a moment $\mathrm{d}\vec{\mu} = -M\mathrm{d}x\mathrm{d}y\mathrm{d}z\hat{\mathbf{z}}$, where M is the magnetization. The force in the z-direction was derived by integrating

over all lower and upper dipoles:

$$F(z) = \frac{2\mu_0 M^2 \delta}{\pi} \frac{1}{a^2+b^2} \Bigg[z \Bigg(a \sinh^{-1}\left(\frac{a}{z}\right) + b \sinh^{-1}\left(\frac{b}{z}\right) - a \sinh^{-1}\left(\frac{a}{B(z)}\right) - b \sinh^{-1}\left(\frac{b}{A(z)}\right) \Bigg) + ab \left(\tan^{-1}\left(\frac{z}{a}\right) - \tan^{-1}\left(\frac{z}{b}\right) \right) - 2a^2 \tan^{-1}\left(\frac{a(\sqrt{a^2+b^2+z^2} - \sqrt{a^2+b^2})}{z(b+\sqrt{a^2+b^2})} \right) - 2b^2 \tan^{-1}\left(\frac{b(\sqrt{a^2+b^2+z^2} - \sqrt{a^2+b^2})}{z(a+\sqrt{a^2+b^2})} \right) \Bigg]. \quad (4)$$

Here, $A(z) = \sqrt{a^2+z^2}$ and $B(z) = \sqrt{b^2+z^2}$, and a, b, and δ are the rail's width, length, and thickness, respectively. The detailed derivation of the force is given in Appendix B

The equilibrium condition was determined by balancing the magnetic force with the total gravitational force:

$$F(z) = (m + m_0)g. \quad (5)$$

To validate the model, we fitted the experimental data using a linear regression of the form $\hat{m}_i = p\tilde{F}(z_i) + q$, where p and q are fitting parameters. The results are shown in Fig. 2.

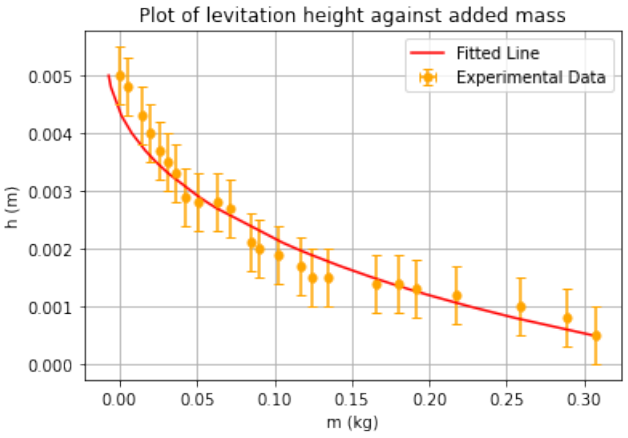

Figure 2. Experimental data and fitted curve $h(m)$

The fitted curve closely matches the experimental data, accurately capturing the non-linear decrease in levitation height with increasing mass. This indicates that the model reflects the underlying physical relationships within the experimental uncertainty.

4. THEORETICAL FRAMEWORK FOR A REAL-WORLD TRAIN

4.1. *Mathematical model of the EDS system*

We are interested in constructing a simple mathematical model in order to model the levitation of the Shinkansen L0 series.

We know that our system comprises of the following elements:

- The train has on each of its sides a row of superconducting coils
- All the vehicle coils are at the same height as well as having the same shape and size
- Two vehicle coils next to each other have currents in opposite directions
- The guideway is made of juxtaposed coils which are shaped as eights
- No current is forced in the guideway coils

In addition, since the train and guideway have a plane of symmetry, we will study the system composed of one side of the train and the guideway next to it.

To facilitate analytical solutions we consider the vehicle coils as perfect circles and treat their magnetic field as that of a magnetic dipole. The current in the vehicle coils is assumed to be fixed, neglecting the effect of induction from the guideway coils. The guideway coils, shaped like eights, are modeled as two circular loops with opposing currents, allowing their magnetic fields to be treated as dipoles. Further assumptions include considering the magnetic field variation over the guideway as minimal due to distance, neglecting boundary effects due to the train's length and assuming the train moves at a constant speed.

We can now model the system as in Figure 3.

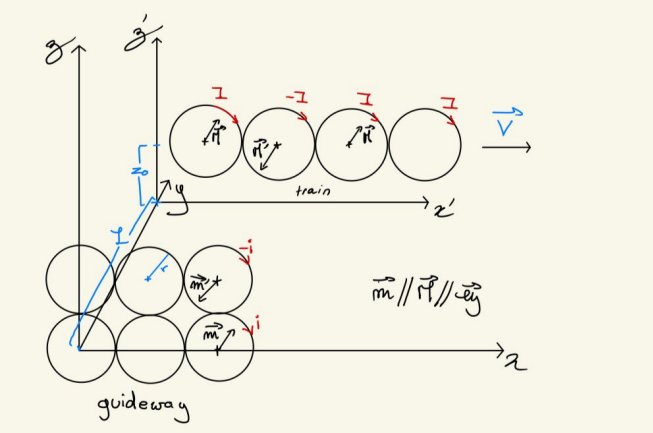

Figure 3. Diagram of the system

Note that, in the above diagram we have taken multiple conventions which we will keep during the derivation:

- All the currents are taken with the axis of the coil equal to the y axis, that is with clockwise direction in our diagram.
- The normal to the surface of all the loops is in the $\hat{\mathbf{e}}_y$ direction.
- The ground is at $z = -r$

The model, being built specifically for the study of levitation, cannot be used for stability nor propulsion.

4.2. Energy analysis

We now want to determine the potential energy of the system as a function of the height of the train to study the potential well.

The total energy of the train will be the sum of the energies associated with each of its coils, given by the formula:

$$U_{\text{mag}} = -\mathbf{M} \cdot \mathbf{B}_{\text{guideway}} \tag{6}$$

With $\mathbf{M} = \pm I\pi R^2 \hat{\mathbf{e}}_y$, being the magnetic moment of the dipole modeling a coil of the train, which depends on the orientation of the coil's current. $\mathbf{B}_{\text{guideway}}$ will be a superposition of many dipole fields:

$$\mathbf{B}(\mathbf{d}) = \frac{\mu_0}{4\pi}\left(\frac{3(\mathbf{m}\cdot\mathbf{d})\mathbf{d}}{d^5} - \frac{\mathbf{m}}{d^3}\right) \tag{7}$$

Here d denotes the distance, $\mathbf{d}$ the position vector with the dipole on the origin.

The magnetic moment of the current loop is given by $|\mathbf{m}| = \pi r^2 I$, with r the radius of the coil of the guideway, and the current i of any arbitrary guideway coil is given by the following formula:

$$i = -\frac{1}{R_e}\frac{d\phi}{dt} \tag{8}$$

Where ϕ is the magnetic flux through the surface enclosed by the coil, and R_e the resistance of the coil.

Considering a guideway coil with its lower loop centered on the origin. One gets the magnetic field of an arbitrary vehicle coil with (3). Using Stokes' theorem, §One can integrate the magnetic potential over the boundary of a guideway loop and find the flux to be:

$$\phi_R = \left(-(2d + p^2(r-d))\frac{E(p)}{1-p^2} + \frac{2dK(p)}{p^2}\right) \times \frac{\mu_0 M_k}{8\pi}\frac{p}{\sqrt{r}d^{\frac{3}{2}}} \tag{9}$$

with p, d, $E(p)$ and $K(p)$ having the following form:

$$d = \sqrt{(x_c - x_k')^2 + (z_c - z_0)^2} \tag{10}$$

$$p^2 = \frac{4rd}{L^2 + (d+r)^2} \tag{11}$$

$$K(p) = \int_0^{\frac{\pi}{2}} \frac{d\alpha}{\sqrt{1 - p^2 m^2 \alpha}} \tag{12}$$

$$E(p) = \int_0^{\frac{\pi}{2}} \sqrt{1 - p^2 m^2 \alpha}\, d\alpha \tag{13}$$

Where L is the distance between the train and the guideway. It is then straightforward to get the total flux through one shaped coil by summing over the flux generated by every vehicle coil through both the bottom and top loops.

When simulating for $\dot{z_0} = 0$ fixed, we find that the current behaves similarly to a sinus function. As shown in the following graph, the two curves superimpose, with an error of only 9×10^{-4}.

Thus, for the rest of the derivation, we will assume that the current is of the form $i = I_0 \sin(\omega t + \phi_0)$ where both I_0 and ϕ_0 are to be determined by simulation.

Finally we can express the magnetic field induced by the guideway as:

$$B_{\text{tot}} = \sum B_{\text{i bottom dipole}} + \sum B_{\text{i top dipole}} \tag{14}$$

We are only interested in the z direction so using the superposition principle and equation (7), we obtain:

$$B_{z,\text{tot}} = \sum_i \frac{\mu r^2}{4}\left[\left(\frac{3L^2}{{d_i}^5} - \frac{1}{{d_i}^3}\right) - \left(\frac{3L^2}{{d_i'}^5} - \frac{1}{{d_i'}^3}\right)\right] \times I_0 \sin\left(\omega t - \phi_0 - \frac{2\omega R(i-1)}{v}\right) \tag{15}$$

with d_i and d_i' being:

$$d_i = \sqrt{z^2 + L^2 + (2r(i-1)\mathbf{e_x} + \mathbf{r_c})^2} \tag{16}$$

$$d_i' = \sqrt{(2r - z)^2 + L^2 + (2r(i-1)\mathbf{e_x} + \mathbf{r_c})^2} \tag{17}$$

Using (6) we can derive the expression for the energy.

5. RESULTS

5.1. Experimental Outcomes and Theoretical Correlation

Our experiment and theoretical analysis have culminated in significant findings regarding the electromagnetic suspension (EMS) capabilities of the Maglev system.

As seen in Figure 2 the fit is particularly close to the values between 0.03 and 0.30 kg of added mass. However between 0 and 0.4 the data point seem to decrease in a linear way. In fact, for the three first points, the fit gives a value out of the error bars. Finally after 0.30 kg, we observe a sharp drop in the train's altitude not modeled by our fit, which continues decreasing until it reaches zero but in a convex manner.

We know from the director of Iran Maglev Technology (IMT) Dr. Hamid Yaghoubi's article in the Journal of Engineering that "In EMS system, the vehicle is levitated about 1 to 2 cm above the guideway using attractive forces" (Yaghoubi 2013). Therefore, we numerically solve $h(m) < h_c = 1cm$ by taking the parameters of a real train i.e. $a = 0.06$m, $b = 153$m, $\delta = 0.0014$m, and $m_0 = 20.10^3$kg.

In this configuration, we obtain a critical mass of 7.5×10^4 kg which corresponds to 941 people with an average mass of 80 kg. This result is close to the maximum capacity of the Shanghai EMS Maglev train, i.e. 959 passengers according to China Discovery (2023), which may serve as a validation of the model when adjusted to reflect practical conditions, confirming that the theoretical predictions can indeed mirror practical outcomes when all relevant factors are considered.

5.2. *Application of the EDS model*

We want to use the theoretical model constructed in the previous part in order to study the levitation of the EDS maglev train. We first start with the constants from the L0 series representing a realistic scenario (Université Paris Saclay) (Wikipedia: L0 Series), and then look at limit cases.

We find that the current is perfectly fitted by a sine function. The mean squared relative error between our current function and the sine fit being 8.4×10^{-5}. This justifies using the assumption $i = I_0 sin(\omega t + \phi_0)$, with the following values:

$$I_0 = 23317.71 \Big| \omega = \frac{2\pi v}{4R} = 598.40 \Big| \phi = 0.0029$$

We can then plot the magnetic field for a speed of $580km/h$, near its top speed:

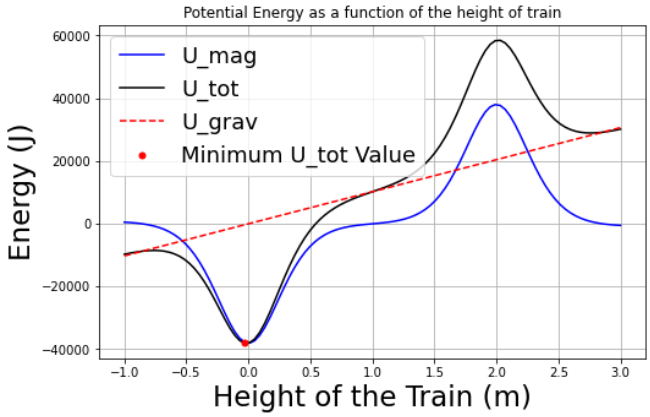

Figure 4. Potential Energy per vehicle coil as a function of the height of the train

Where we find an equilibrium position at $z_0 = -0.030m$, meaning the center of the train's coils are at $0.970m$ above ground, since the radius of the coil in the guideway is $1m$.

Now we are interested in the behavior of our model in limit cases: whether it behaves as expected and under what conditions it presents limitations. Here the current does not behave as a sine anymore, so we drop the assumption.

First we focus on small velocities. At very low velocities, while there is still a magnetic field shown in Figure 7, the magnetic energy is too small to compensate the gravitational one, and there is no stable equilibrium. In fact we find that as soon as the speed is lower than $25m.s^-1$ the train has no levitation point.

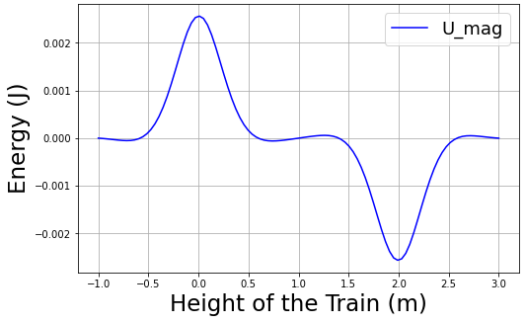

Figure 5. Magnetic field by the guideway at the center of a vehicle coil for $v = 1m.s^{-1}$

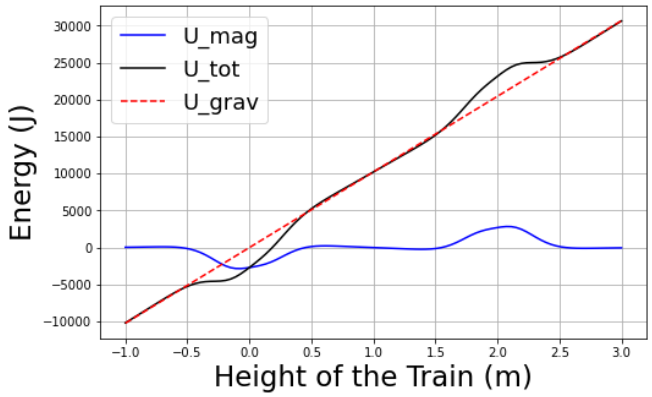

Figure 6. Potential energy for v = 25 m.s^{-1}

The mass of the train has a similar role. Increasing the mass of the train does not change the magnetic energy but increases the slope of the gravitational energy. Thus there is a threshold value above which the train can not levitate. It is of 150 tonnes per car, high above the value of an unloaded car: 25 tonnes.

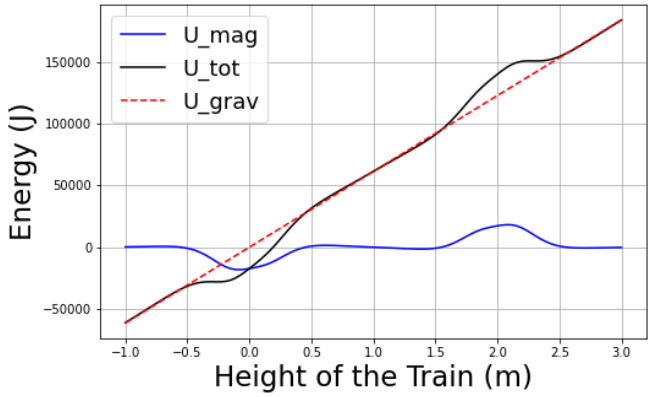

Figure 7. Potential energy for $m = 150$

6. DISCUSSION

To quantitatively assess the accuracy of our fit in predicting levitation heights based on varying masses, we calculate the coefficient of determination, denoted R^2, which yields an accuracy score of 96.0%. This result is encouraging, yet certain regions reveal limitations in the fit's effectiveness.

However, the high uncertainty in the data, mainly due to the 1 mm uncertainty of the ruler used for measurement, complicates the evaluation of the fit's correspondence with the observed data.

Regarding the accuracy of our fit, we approximated the system by assuming negligible forces between diagonal magnets and considering all four magnets as identical. Since the experiment itself was an approximation of a maglev train, our fit cannot fully capture the train's behavior, especially under conditions where the system's assumptions become inadequate—such as when the train is in close proximity to the guideway.

For what is of the mathematical model we developed, Figure 4 indicates that levitation occurs at approximately a meter from the ground. Indeed, z_0 represents the height of the center of the vehicle coils. Thus the bottom of the train is more than R under the value of z_0. In fact, assuming that there are about 20 to 40 cm of layers of metals under the coil, the underside of the train is 10 cm above the ground. This is indeed how the Shinkansen behaves in real life. However, some constants of the L0 series are not directly available in open sources and were thus estimated.

Regarding the limit cases, they also behave as expected. For the train to levitate, we need the force associated to the magnetic field to be greater than that of the gravity: $f_{\text{mag}} > mg$ and f_{mag} is a strictly increasing function with v, thus for the train to levitate we need that $\text{v} > f_{\text{mag}}^{-1}(mg)$. That is there is a threshold value of speed under which the train cannot levitate. We know that for the real train this value is around 100km/h. Thus our result, which is 90 km.h^{-1}, is very close. Equivalently, we need that $f_{\text{mag}}/g > m$. With the constants used we had $f_{\text{mag}}/g = 150$ tonnes per car.

7. CONCLUSION

7.1. *Limitations of the fit of the experiment*

We found that the fit diverges from the experimental data in the interval $(0, 0.03)$ kg and for values above 0.30 kg. The linear behavior of the data points under 0.03 kg of added mass can be understood by noting that $m \ll m_0$, so the change in height induced by adding m to the train will result in a change in height $z \ll z_0$. If $H(m)$ is the true function giving the height of the train as a function of m, close to 0 we have

$$H(m) = h_0 + m\frac{dh}{dm},$$

which indicates that the height of the train decreases linearly with the added mass. However, this is not accounted for by our fit, as the function F does not depend on the mass.

Similarly, for masses above 0.3 kg, the height decreases sharply. This suggests a maximum in the magnetic force, beyond which the gravitational force prevents the train from levitating. Once again, this behavior is not captured by our fit. Firstly, it was derived under the assumption that the magnets are composed of infinitesimal magnetic dipoles. Two magnetic dipole create a force which goes to infinity when they get closer. In our case since the dipole are infinitesimal they create a force with finite maximum

but which still increases drastically when the magnets are pulled together, thus explaining the convex profile of our fit. Secondly, we assumed that the height of the train is much larger than the thickness of the magnet, which is not true for $m > 0.3kg$.

7.2. *Limitations of the mathematical model of the EDS system*

When simulating the behavior of the system at very high speed we found:

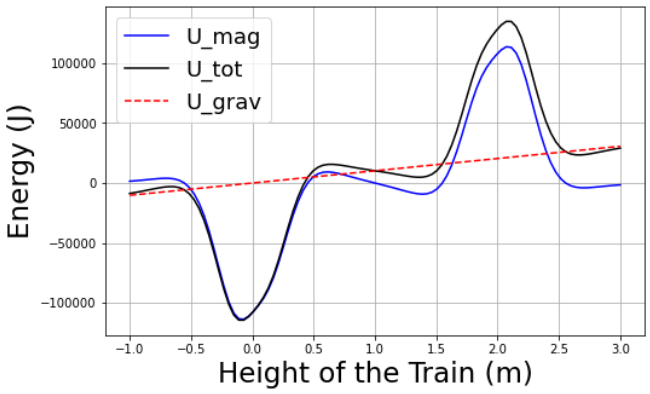

Figure 8. Potential energy for v = 1000 m.s^{-1}

This is not what is expected. The maglev train cannot go over 650 km.h^{-1} despite our results showing an equilibrium point. This inconsistency is due to the limitations of our system. Indeed, our model does not take into consideration the mechanisms associated with propulsion.

Firstly, we considered that the magnetic field used for propulsion does not impact the levitation. This was justified as this magnetic field should create a force in the $\hat{e}_x$ direction, thus not impacting the $\hat{e}_y$ direction. However, at speeds over 650 km.h^{-1}, this magnetic field is extremely large, hence its $\hat{e}_y$ component is not negligible anymore. it could be responsible for a loss of levitation, or stability, preventing the train from accelerating above 650 km.h^{-1}.

Secondly, it is also possible that the propulsion mechanisms do not have the capacity of propelling the train at such a speed. Then the error would be that we assumed that reaching such a speed was possible.

REFERENCES

H. Yaghoubi, Journal of Engineering **2013**, Article ID 537986, 19 pages (2013).

C. Discovery, "Shanghai maglev train," https://www.chinadiscovery.com/shanghai/shanghai-maglev.html (2023).

Université Paris Saclay, "Applications train maglev," https://hebergement.universite-paris-saclay.fr/supraconductivite/supra/en/applications-trains-maglev-more.php.

Wikipedia: L0 Series, https://en.wikipedia.org/wiki/L0$_{S}eries$.

APPENDIX A: EXPERIMENTAL DATA

Table 1. Experimental data for the mass (m) and levitation height (h) of the Maglev train model. The uncertainties are ±1 g for m and ±0.5 mm for h.

m (g)	h (mm)
0	5.0
5	4.8
15	4.3
20	4.0
26	3.7
31	3.5
36	3.3
43	2.9
51	2.8
63	2.8
71	2.7
85	2.1
90	2.0
103	1.9
117	1.7
124	1.5
135	1.5
166	1.4
180	1.4
192	1.3
217	1.2
259	1.0
289	0.8
307	0.5
322	0.0

APPENDIX B: ANALYTICAL DERIVATION OF THE FORCE INDUCED BY THE DIPOLE MOMENT

In this section, we derive the expression for the magnetic force $F(z)$ acting on a Maglev train system, modeled as layers of magnetic dipoles. The approach follows the calculations shown in the handwritten derivation, and includes step-by-step integration over the magnetic fields produced by the rails.

We model each rail as a continuous surface distribution of magnetic dipoles. Let M be the surface magnetization of the rail, oriented along the z-axis. The infinitesimal dipole moment of an element of the rail is defined as:

$$d\vec{\mu} = M\, dx'\, dy'\, \vec{e}_z,$$

The objective is to compute the magnetic force between two layers of dipoles (representing the upper and lower rails) as a function of the distance z between them.

The magnetic vector potential $\vec{A}$ at a point $\vec{r} = (x, y, z)$ due to an infinitesimal surface dipole element is given by:

$$d\vec{A}(\vec{r}) = \frac{\mu_0 M}{4\pi} \frac{d\vec{\mu} \times (\vec{r} - \vec{r'})}{|\vec{r} - \vec{r'}|^3}$$

$$d\vec{A}(\vec{r}) = \frac{\mu_0 M}{4\pi} \frac{dx'dy'}{[(x-x')^2 + (y-y')^2 + z^2]^{3/2}} \begin{bmatrix} -(y-y') \\ x - x' \\ 0 \end{bmatrix},$$

where μ_0 is the permeability of free space ($\mu_0 = 4\pi \times 10^{-7}\,\mathrm{N/A^2}$).

To find the total vector potential generated by the lower rail of dimensions $a \times b$, we integrate over the entire top rail surface:

$$\vec{A}(\vec{r}) = \frac{\mu_0 M}{4\pi} \int_{x-a}^{x} \int_{y-b}^{y} \frac{dXdY}{[X^2 + Y^2 + z^2]^{3/2}} \begin{bmatrix} -Y \\ X \\ 0 \end{bmatrix}.$$

where we did the change of variable $X = x - x', Y = y - y'$.

We derive the integrals necessary for computing the magnetic potential and force in the system. The integrals will be evaluated over the specified ranges using the correct variables dX and dY.

$$I_0(X) = \int_{y-b}^{y} \frac{YdY}{(X^2+Y^2+z^2)^{3/2}}) = \left[\frac{1}{\sqrt{X^2+Y^2+z^2}}\right]_{Y=y-b}^{y}$$

$$I_1(Y) = \int_{x-a}^{x} \frac{XdX}{(X^2+Y^2+z^2)^{3/2}}. = \left[\frac{1}{\sqrt{X^2+Y^2+z^2}}\right]_{X=x-a}^{x}.$$

$$I_2 = \int_{x-a}^{x} I_0(X)dX = \left[\ln\left(\frac{\sqrt{X^2+y^2+z^2}+X}{\sqrt{X^2+(y-b)^2+z^2}+X}\right)\right]_{X=x-a}^{x}$$

$$I_3 = \int_{y-b}^{y} I_1(Y)dY = \left[\ln\left(\frac{\sqrt{(x-a)^2+Y^2+z^2}+Y}{\sqrt{x^2+Y^2+z^2}+Y}\right)\right]_{Y=y-b}^{y}.$$

From there, one gets the full expression of the vector potential $\vec{A}(\vec{r})$:

$\vec{A}(\vec{r}) =$

$$\frac{\mu_0 M}{4\pi} \begin{pmatrix} \ln\left(\frac{\sqrt{(y-b)^2+z^2+(x-a)^2}+(x-a)}{\sqrt{(y-b)^2+z^2+x^2}+x} \frac{\sqrt{y^2+z^2+x^2}+x}{\sqrt{y^2+z^2+(x-a)^2}+(x-a)}\right) \\ \ln\left(\frac{\sqrt{(y-b)^2+z^2+x^2}+(y-b)}{\sqrt{y^2+z^2+x^2}+y} \frac{\sqrt{y^2+z^2+(x-a)^2}+y}{\sqrt{(y-b)^2+z^2+(x-a)^2}+(y-b)}\right) \\ C \end{pmatrix}.$$

The magnetic field $\vec{B}$ can be derived from the vector potential $\vec{A}$ using the relation:

$$\vec{B} = \nabla \times \vec{A}.$$

However, due to the symmetry of the system, only the z-component of the magnetic field is significant for our analysis. Thus, we focus on calculating B_z, which is given by:

$$B_z = \frac{\partial A_y}{\partial x} - \frac{\partial A_x}{\partial y}.$$

The upper rail, positioned at a height z, consists of a layer of dipole moments aligned downward:

$$d\vec{\mu} = -M\,dx\,dy\,\vec{e}_z.$$

The force on each dipole in the presence of a magnetic field is given by:

$$d\vec{F} = \nabla(d\vec{\mu} \cdot \vec{B}).$$

To find the total force on both upper rails by both lower rails, we integrate over its surface. The z-component of the force is:

$$F(z) = -2M \int_0^a \int_0^b \partial_z B_z(z) dxdy.$$

$$F(z) = -2M \int_0^a dx \int_0^b \partial_z(\partial_x A_y - \partial_y A_x) dy.$$

$$F(z) = -2M \frac{\partial}{\partial z} \left(\int_0^b [A_y]_{x=0}^{a} dy - \int_0^a [A_x]_{y=0}^{b} dx \right).$$

Using the identities:

$$\sinh^{-1}(U) = \ln(\sqrt{1+U^2} + U)$$

and

$$\int_0^{U_{max}} \sinh^{-1}(\frac{U}{U_0})dU = U_{max}\sinh^{-1}(\frac{U_{max}}{U_0}) - \sqrt{U_0^2 + U_{max}^2} + U_0$$

, we obtain the following expression of the induced force along the z-axis:

$$F(z) = -\frac{2\mu_0 M^2}{\pi} \frac{\partial \Phi}{\partial z}(z)$$

where Φ, defined below, is a dimensionless potential for the force:

$$\Phi(z) = a\sinh^{-1}(\tfrac{a}{z}) + b\sinh^{-1}(\tfrac{b}{z}) - a\sinh^{-1}(\tfrac{a}{B(z)}) - b\sinh^{-1}(\tfrac{b}{A(z)}) - 2(A(z)+B(z)) + 2(z + \sqrt{a^2+b^2+z^2}) \quad \text{(B1)}$$

With $A(z) = \sqrt{a^2 + z^2}$ and $B(z) = \sqrt{b^2 + z^2}$

To extend our results to a more realistic 3D scenario, we consider the finite thickness δ of the upper rail. The magnetic field correction can be approximated as:

$$F^{(3D)}(z) \propto \frac{\partial B_z^{(3D)}}{\partial z} \approx B_z^{(2D)}(z+\delta) - B_z^{(2D)}(z).$$

This approximation accounts for the finite thickness of the magnetic layers and provides a more accurate representation of the force. We proceed as follows:

First, we consider an elementary dipole moment $d\vec{\mu} = -M_{3D} dx dy dz \vec{e_z}$ where $M_{3D} = \frac{M_{2D}}{\delta}$ is the magnetization in A/m can be defined as density of dipole moment per unit volume.

$$\vec{F} = 2\int_0^a \int_0^b \int_{z_0}^{z_0+\delta} \nabla(d\vec{\mu} \cdot \vec{B}).$$

Since we are only interested in F_z by symmetry, we proceed:

$$F_z(z) = -2M_{3D} \int_0^a \int_0^b \int_{z_0}^{z_0+\delta} B_z^{3D}(z)\; dx\, dy\, dz.$$

Expanding further, using the approximation above:

$$F_z = -2M_{3D} \int_{z_0}^{z_0+\delta} \int_0^b \int_0^a \left(\frac{\partial}{\partial z} \int_0^\delta B_z^{2D}(z-z')\, dz' \right) dx dy dz.$$

$$F_z = \frac{1}{\delta} \int_{z_0}^{z_0+\delta} dz \int_z^{z-\delta} dz' \left(\int_0^a \int_0^b -2M \partial_z B_z^{(2D)}(z)\, dx\, dy \right).$$

On the other hand, we recognize the force expression we had using the zero-thickness model (i.e. in two dimensions):

$$F_z^{(2D)} = -2\int_0^b \int_0^a M_{2D}\, dx\, dy\, \partial_z B_z^{(2D)}(z).$$

Thus:

$$F_z = \frac{1}{\delta} \int_{z_0}^{z_0+\delta} dz \int_{z-\delta}^{z} \left[F_z^{(2D)}(z') \right] dz'.$$

$$F_z = -\frac{2\mu_0 M_{3D}^2 \delta}{\pi} \int_{z_0}^{z_0+\delta} dz \int_{z-\delta}^{z} \left[\frac{\partial \Phi}{\partial z}(z') \right] dz'.$$

Given a position z_0 below the top rail, we have:

$$F_z(z_0) = -\frac{2\mu_0 M_{3D}^2 \delta}{\pi} \int_{z_0}^{z_0+\delta} (\Phi(z-\delta) - \Phi(z))\, dz$$

We define the primitive Ψ of Φ:

$$\Psi(z) = \int \Phi(z)\, dz.$$

Step-by-Step Derivation:

$$J_0 = \int a \, \sinh^{-1}(\frac{a}{z})\, dz.$$

$$J_0 = a\, z \, \sinh^{-1}(\frac{a}{z}) + a^2 \ln\left(z + \sqrt{a^2+z^2} \right).$$

$$J_1 = \int b \, \sinh^{-1}(\frac{b}{z})\, dz.$$

$$J_1 = b\, z \, \sinh^{-1}(\frac{b}{z}) + b^2 \ln\left(z + \sqrt{b^2+z^2} \right).$$

$$J_2 = \int -a \, \sinh^{-1}(\frac{a}{B(z)})\, dz.$$

$$J_2 = -a\, z \, \sinh^{-1}(\frac{a}{B(z)}) + 2a^2 \arctan\left(\frac{z}{\sqrt{a^2+b^2}} \right).$$

$$J_3 = \int -b \, \sinh^{-1}(\frac{b}{A(z)})\, dz.$$

$$J_3 = -b\, z \, \sinh^{-1}(\frac{b}{A(z)}) + 2b^2 \arctan\left(\frac{z}{\sqrt{a^2+b^2}} \right).$$

$$J_4 = \int -2\big(A(z) + B(z)\big)\, dz$$

$$J_4 = -\left[z\sqrt{a^2+z^2} + a^2 \sinh^{-1}\left(\frac{z}{a}\right) \right] - \left[z\sqrt{b^2+z^2} + b^2 \sinh^{-1}\left(\frac{z}{b}\right) \right]. \quad \text{(B2)}$$

$$J_5 = \int 2\left(z + \sqrt{a^2+b^2+z^2} \right)\, dz$$

$$J_5 = z^2 + z\sqrt{a^2+b^2+z^2} + (a^2+b^2) \sinh^{-1}\left(\frac{z}{\sqrt{a^2+b^2}} \right).$$

So, by combining all terms, the final expression for $\Psi(z)$ is:

$$\begin{aligned}\Psi(z) = a\,z\,\sinh^{-1}(\frac{a}{z}) + b\,z\,\sinh^{-1}(\frac{b}{z}) \\ - a\,z\,\sinh^{-1}(\frac{a}{B(z)}) - b\,z\,\sinh^{-1}(\frac{b}{A(z)}) \\ - z\sqrt{a^2+z^2} - a^2\sinh^{-1}\left(\frac{z}{a}\right) \\ - z\sqrt{b^2+z^2} - b^2\sinh^{-1}\left(\frac{z}{b}\right) \\ + z^2 + z\sqrt{a^2+b^2+z^2} + (a^2+b^2)\sinh^{-1}\left(\frac{z}{\sqrt{a^2+b^2}}\right).\end{aligned} \tag{B3}$$

Hence, we obtain an expression of F_z the force induced by the magnetic dipole moment on the top rails along the z-axis:

$$F_z(z_0) = \frac{2\mu_0 M_{3D}^2 \delta}{\pi(a^2+b^2)}(\Psi(z_0+\delta) + \Psi(z_0-\delta) - 2\Psi(z_0))$$

Then, we generalize to an arbitrary position z between the two rails, drop the 2D/3D indices, consider $\delta/z << 1$ and find:

$$\begin{aligned}F(z) = \frac{2\mu_0 M^2 \delta}{\pi}\frac{1}{a^2+b^2}\Bigg[z\Bigg(a\sinh^{-1}\left(\frac{a}{z}\right) + b\sinh^{-1}\left(\frac{b}{z}\right) \\ - a\sinh^{-1}\left(\frac{a}{B(z)}\right) - b\sinh^{-1}\left(\frac{b}{A(z)}\right)\Bigg) \\ + ab\left(\tan^{-1}\left(\frac{z}{a}\right) - \tan^{-1}\left(\frac{z}{b}\right)\right) \\ - 2a^2\tan^{-1}\left(\frac{a(\sqrt{a^2+b^2+z^2} - \sqrt{a^2+b^2})}{z(b+\sqrt{a^2+b^2})}\right) \\ - 2b^2\tan^{-1}\left(\frac{b(\sqrt{a^2+b^2+z^2} - \sqrt{a^2+b^2})}{z(a+\sqrt{a^2+b^2})}\right)\Bigg].\end{aligned} \tag{B4}$$